J. Chem. Sci. Vol. 128, No. 7, July 2016, pp. 1131–1140.
DOI 10.1007/s12039-016-1115-z

Amine-functionalized magnetic nanoparticles as robust support for immobilization of Lipase

BANALATA SAHOO, SUJAN DUTTA and DIBAKAR DHARA*

Department of Chemistry, Indian Institute of Technology Kharagpur, Kharagpur, West Bengal 721302, India
e-mail: dibakar@chem.iitkgp.ernet.in; dibakar@live.in

MS received 10 January 2016; revised 8 April 2016; accepted 9 May 2016

Abstract. Preparation of magnetic nanoparticles with controlled size and shape along with modulation of their surface properties *via* introduction of functional groups holds great prospect in the field of nanotechnology. Superparamagnetic, aqueous dispersible iron oxide nanoparticles (Fe_3O_4) with amine-functionalized surface were prepared through solvothermal method, using poly(ethylene imine) (PEI), ethanolamine (EA), and 2,2′-(ethylenedioxy)bis(ethylamine) (EDBE) as amine precursors. These aminated nanoparticles were used as support for the immobilization of lipase, an important industrial enzyme. Lipase was immobilized *via* glutaraldehyde coupling agent. These functionalized nanoparticles were characterized by XRD, FTIR, TEM, FESEM and VSM analysis. The maximum activity was obtained for the lipase immobilized on EDBE modified Fe_3O_4 nanoparticles. The lipase immobilized on EDBE-Fe_3O_4 depicted 83.9% relative activity with respect to the same amount of free lipase. Moreover, lipase immobilized on EDBE-Fe_3O_4 nanoparticles demonstrated good thermal and storage stability, and easy reusability. The kinetic parameters of lipase immobilized on EDBE-Fe_3O_4 were compared with those of free lipase and the apparent Michaelis-Menten constant of immobilized lipase was found to be nearly same as that of free lipase.

Keywords. Biomaterials; enzyme activity; enzyme biocatalysis; nanoparticles; surface properties.

1. Introduction

The immobilization of enzymes and proteins on nanoparticles resulting in improved catalytic properties has led to increased importance of these biocatalysts.[1,2] The immobilization of enzymes on nanoparticles have several important benefits compared to conventional supports due to their higher enzyme loading capacity and significantly enhanced mass transfer efficiency.[3] Enzyme immobilization results in improved storage stability, operational stability and facilitates continuous bioprocess in industry.[4,5] The success of enzyme immobilization mainly relies on the nature of the solid support used. The inorganic nanomaterials provide superior support for enzymes than organic ones as they provide high stability of enzyme, high resistance to microbial corrosion, and better reusability.[6]

Among inorganic nano-materials chosen for enzyme immobilization, magnetic nanoparticles (MNPs) are the most widely accepted carriers of proteins/enzymes, owing to the ease of recovery of the substrate and product.[7,8] Magnetic bio-separation strategy provides an easy way of isolation of a product from the enzyme-immobilized magnetic particles with the assistance of a simple magnet. However, the generation of well-dispersed and surface-functionalized MNPs is the key challenge of current in spite of several methods for the synthesis of amine-functionalized MNPs are reported.[9–12] To generate amine-functionalized MNPs, Hritcu *et al.,* prepared MNPs dispersed in chitosan microspheres.[9] The average size for magnetic-chitosan composite nanoparticles obtained in this method was too high (40 μm) which is very difficult to use further in biological field. Xie *et al.*,[12] prepared amine-functionalized MNPs using (3-aminopropyl) triethoxysilane using post surface modification. The obtained amine-MNPs were not discrete and well shaped as evident from TEM images. Chen *et al.*,[13] have sucessfully synthesized amine-functionalized Fe_3O_4@C nanoparticles on a large scale and demonstrated the potential of these nanoparticles as a platform for lipase immobilization. So, there is a continuous need for finding out newer ways to make amine-MNPs which can be utilized for further surface modifications. In the present work, a single step, facile method has been developed to produce stable amine-functionalized Fe_3O_4 nanoparticles using different amine precursors such as branched poly(ethylene imines) (PEI), 2,2′-(ethylenedioxy)bis(ethylamine) (EDBE) and ethanolamine (EA).

*For correspondence

One of the important use of the amine-functionalized MNPs is for enzyme immobilization. Of the several enzymes used for immobilization on MNPs,[14–17] lipase has been significantly exploited for immobilization studies owing to its numerous industrial benefits. *Candida rugosa lipase* (CRL) is one of the most important industrial biocatalysts due to its wide spectrum of applications, *e.g.*, in hydrolysis and esterification reactions, and due to its high stereoselectivity and regioselectivity required in the synthesis of several pharmaceuticals.[18] They hydrolyze fats into fatty acids and glycerol at the water-lipid interface and can reverse the reaction in non-aqueous media. Several potential applications of lipase include organic synthesis, bioconversions, resolution of enantiomers, as well as other applications in pharmaceutical, dairy and chemical industries.[19]

So far, many research groups have reported successful conjugation of lipase on different carriers.[20–23] Ren *et al.*, studied polydopamine coated magnetic nanoparticles (PD-MNPs) for immobilization of lipase.[23] Chen *et al.*, have used amine-functionalized Fe_3O_4@C nanoparticles for lipase immobilization.[13] Lee *et al.*,[24] had reported immobilization of lipase on hydrophobic MNPs, lipase was immobilized on magnetic nanoparticles supported ionic liquids.[25] However, there is a need for a simple single-step method for the preparation of amine-functionlized MNPs which can be used for immobilization of lipase. In the present work, preparation of amine functionalized MNPs using a simple chemical approach has been achieved. Further, lipase was immobilized onto these magnetic nanoparticles *via* gluteraldehyde. The enzymatic activity of immobilized lipase has been compared with the free enzymes and discussed. The specific enzymatic activity (U/mg of lipase), Michaelis-Menten kinetic constant (K_m) and thermal stability of immobilized lipase on EDBE-Fe_3O_4 were determined and compared with free lipase in solution. The reusability of the immobilized lipase on magnetic nanoparticles was quantified and found to be encouraging for potential use.

2. Experimental

2.1 *Materials*

Anhydrous ferric chloride ($FeCl_3$), ethanolamine (EA), anhydrous sodium acetate, ethylene glycol, and glutaraldehyde were obtained from Merck, Germany. Branched poly(ethylene imines) (PEI) (MW 25,000), 2,2′-(ethylenedioxy)bis(ethylamine) (EDBE), *p*-nitrophenyl butyrate (PNPB), and Bradford reagent were purchased from Sigma-Aldrich Chemicals, USA. *Candida rugosa lipase* (E.C-3.1.1.3) of two different units (Lot result: 807 U/mg, 2.45 U/mg) were purchased from Sigma-Aldrich Chemicals, USA. All the chemicals were reagent grade and used without further purification. Ultrapure Milli-Q water was used for all the experiments.

2.2 *Synthesis of Amine-Functionalized Fe_3O_4 Nanoparticles*

Amine-functionalized superparamagnetic Fe_3O_4 nanoparticles were prepared by a facile single-step solvothermal method in an autoclave. In this approach, 1.0 g $FeCl_3$ (2 mmol), 3.0 g sodium acetate and 10 mL of respective amine modifying agents (PEI, EDBE and EA) were dissolved in 30 mL ethylene glycol. The resulting mixtures were vigorously stirred at room temperature to get clear transparent solutions. The resulting mixtures were then transferred into a Teflon-lined stainless steel autoclave (50 mL) and heated for 24 h at 160°C. The solutions were then cooled to room temperature and the resulting particles were subjected to magnetic decantation followed by repeated washing with Milli-Q water and drying in a vacuum oven at 70°C.

2.3 *Preparation of Glutaraldehyde-linked Fe_3O_4 Nanoparticles*

The amine-functionalized Fe_3O_4 nanoparticle dispersions were further treated with glutaraldehyde coupling agent. 2 mL of 25% glutaraldehyde was diluted to 20 ml with 0.01 M PBS buffer. The pH of the resulting solution was made 8.0 with dilute NaOH solution. To the above mixture, 50 mg of amine-functionalized MNPs were added. The mixture was sonicated for 30 min and then stirred for another 2 h at room temperature, followed by recovery of the glutaraldehyde-conjugated Fe_3O_4 particles by magnetic separation and thorough washing with PBS buffer for 3–4 times before final recovery.

2.4 *Lipase Immobilization on Fe_3O_4 Nanoparticles*

50 mg of the glutaraldehyde modified Fe_3O_4 nanoparticles (GLU-EDBE-Fe_3O_4, GLU-EA-Fe_3O_4 and GLU-PEI-Fe_3O_4) were treated with 100 μg/mL of lipase in 50 mL 10 mM phosphate buffer solution (pH 7.4) and shaken for 24 h at 27°C. Thereafter, the lipase bound nanoparticles were recovered through magnetic separation, followed by repeated washing with PBS buffer. The dacant lipase after the reaction and washing were recovered to determine the amount of lipase bound to the MNPs.

2.5 *Estimation of Lipase Immobilization*

The concentration of immobilized lipase (a protein) on Fe_3O_4 nanoparticles was determined according to Bradford's method, using a calibration curve obtained from a series of lipase solution of different concentrations.[26]

2.6 *Lipase Activity Assay*

The hydrolytic activity of free lipase and immobilized lipase were monitored spectrophotometrically at 403 nm, using the rate of hydrolysis of a simple substrate *p*-nitro phenyl butyrate (PNPB) according to the procedure followed by Chiou *et al*.[22] In brief, substrate solutions (PNPB) of different concentration ranging from 5.68 mM to 28.44 mM were prepared by dissolving the respective quantities of PNPB in ethanol. For activity studies, 3 mL of PBS, 100 μL of PNPB solution in ethanol (28.4 mM), 20 μL (1 mg mL^{-1}) of free lipase solution or 5 mg of lipase-immobilized nanoparticles were taken in 15 mL eppendorf tube and incubated for 60 min. After that, the reaction was stopped and the absorbance at 403 nm was noted. In the case of the immobilized enzyme, magnetic separation was performed before taking the absorbance measurement. The absorbance recorded was expressed in terms of specific activity from a calibration curve obtained from the absorbance noted for a series of p-nitrophenol solutions of known concentrations in buffer. The specific activity of the enzyme is expressed as follows: micromole of product formed per unit time per mg of protein under the specified experimental conditions.

2.7 *Characterization*

Powder X-ray diffraction (XRD) measurement of the nanoparticles and their modified counterparts were performed by Phillips PW 1710 X-ray diffractometer (XRD) with Ni-filtered Cu-Kα radiation (λ = 1.54 Å). The surface composition and surface functionality of the nanoparticles were revealed by FTIR spectra. Samples for FTIR measurement were prepared in KBr and spectra were recorded in the range 400–4000 cm^{-1}. The lipase activity was obtained by UV-Vis spectrophotometric analysis. The hydrodynamic size of the particles was measured by dynamic light scattering using a Brookhaven 90 Plus particle size analyzer. The size and morphology of the nanoparticles were investigated by high-resolution transmission electron microscopy (HRTEM, JEOL 3010, Japan, operated at 300 kV). The nanoparticles were thoroughly dispersed in water by ultra-sonication and a drop of the solution was placed on carbon coated copper grid. The surface morphology of the nanoparticles was obtained by field emission scanning electron microscopy (FESEM, Phillips CM 200). The average particle size of nanoparticles was determined by using image J software. Thermal analysis was done with a thermal analyzer (Pyris Diamond TG-DTA) with a heating rate 8°C/min in the temperature range 50 to 1000°C. Magnetic nature of nanoparticles was performed using a SQUID-VSM instrument (Evercool SQUID VSM DC Magnetometer). Nitrogen adsorption-desorption measurement was performed to determine surface area, pore volume and pore distribution by using a N_2 adsorption–desorption instrument (Quantachrome Corporation, Quantachrome autosorb automated gas sorption system).

3. Results and Discussion

Superparamagnetic, water dispersible and amine-functionalized Fe_3O_4 nanoparticles of narrow-dispersity were obtained through a single-step inexpensive chemical route. Here, amine precursors served as both capping and surface modifying agent. The detailed procedure for the conjugation of lipase on the amine-functionalized Fe_3O_4 nanoparticles is outlined in Scheme 1. Initially, a yellow colored mixture of $FeCl_3$, sodium acetate and ethylene glycol was transferred to the brown colored amine precursors. On addition of amine modifying agent, iron complex was formed which, upon heating, underwent polycondensation, nucleation and growth to form amine-functionalized Fe_3O_4 nanoparticles. The detailed mechanism for the formation of Fe_3O_4 nanoparticles using polyol method was described by Kwak *et al*.[27]

The amine-derivatized Fe_3O_4 nanoparticles were then treated with glutaraldehyde to produce aldehyde-functionalized (GLU-Fe_3O_4) nanoparticles. The final step involved the immobilization of lipase on the GLU-Fe_3O_4 nanoparticles through an imine bond formation between the amine groups on lipase and the aldehyde groups on the Fe_3O_4 nanoparticles.

3.1 *X-Ray Diffraction Analysis*

The formation of Fe_3O_4 nanoparticles, their crystallinity and phase purity were verified by XRD analysis. The wide-angle XRD patterns of aminated Fe_3O_4 are presented in Figure 1. The XRD patterns of amine-functionalized nanoparticles were compared with the pristine Fe_3O_4 nanoparticles synthesized through the same method. In the XRD pattern of EDBE-Fe_3O_4 and

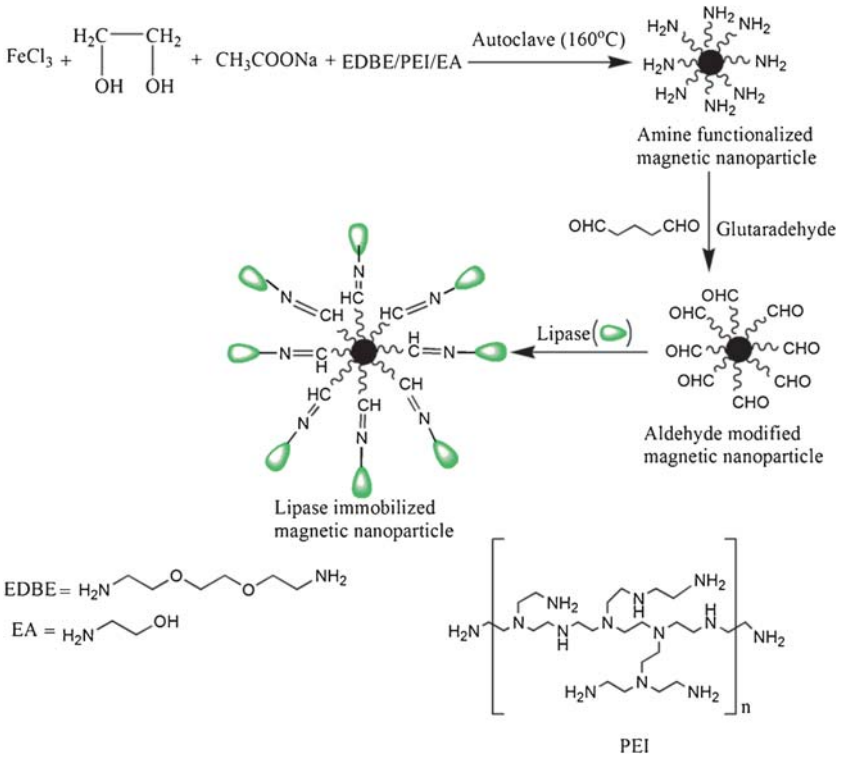

Scheme 1. Schematic presentation of the preparation of amine-functionalized MNPs and covalent conjugation of lipase.

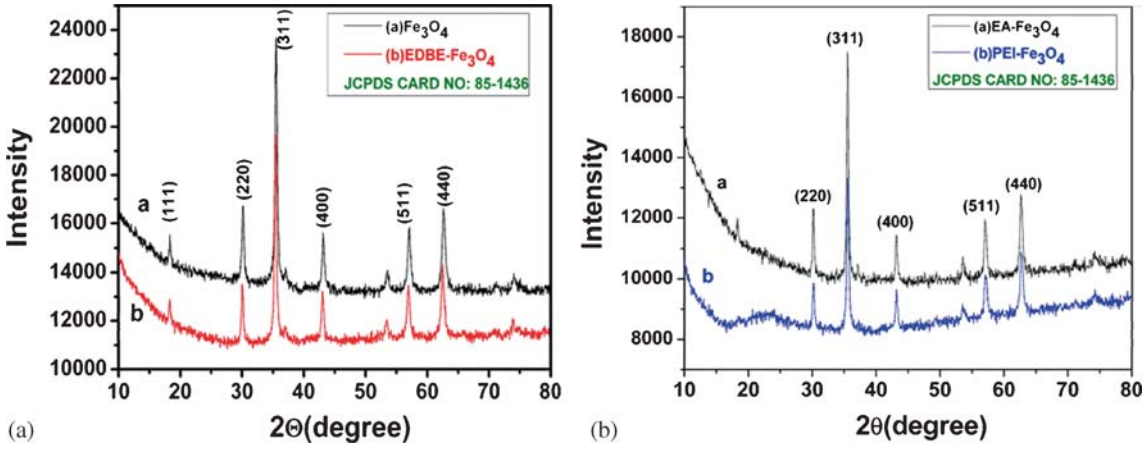

Figure 1. X-ray diffraction pattern of (a) Pristine Fe_3O_4 and EDBE-Fe_3O_4 nanoparticles, (b) EA-Fe_3O_4 and PEI-Fe_3O_4.

free Fe_3O_4 nanoparticles (Figure 1a), peaks at angles 18.29°, 30.09°, 35.44°, 43.07°, 56.96°, 62.55° correspond to (111), (220), (311), (400), (511), and (440) Bragg's diffraction planes respectively, which corroborates with the XRD pattern of pristine Fe_3O_4 nanocrystals. In Figure 1b, for PEI-coated Fe_3O_4 nanoparticles (PEI-Fe_3O_4), a broad peak is observed at an angle between 20–25° which can be assigned to the PEI polymer modification on Fe_3O_4 nanoparticles. The position and relative intensities of all XRD peaks have been matched with the standard diffraction pattern of pure Fe_3O_4 nanoparticles (according to JCPDS card no. 85-1436). The absence of any undesired peaks in the XRD pattern clearly conveys the purity of the prepared nanoparticles.

3.2 *FTIR Measurement*

Surface functionalization of the nanoparticles was analyzed by FTIR spectroscopy. The FTIR spectra of the amine-functionalized Fe_3O_4 and the free Fe_3O_4 nanoparticles obtained through solvothermal method are displayed in Figure 2. The FTIR spectra of free

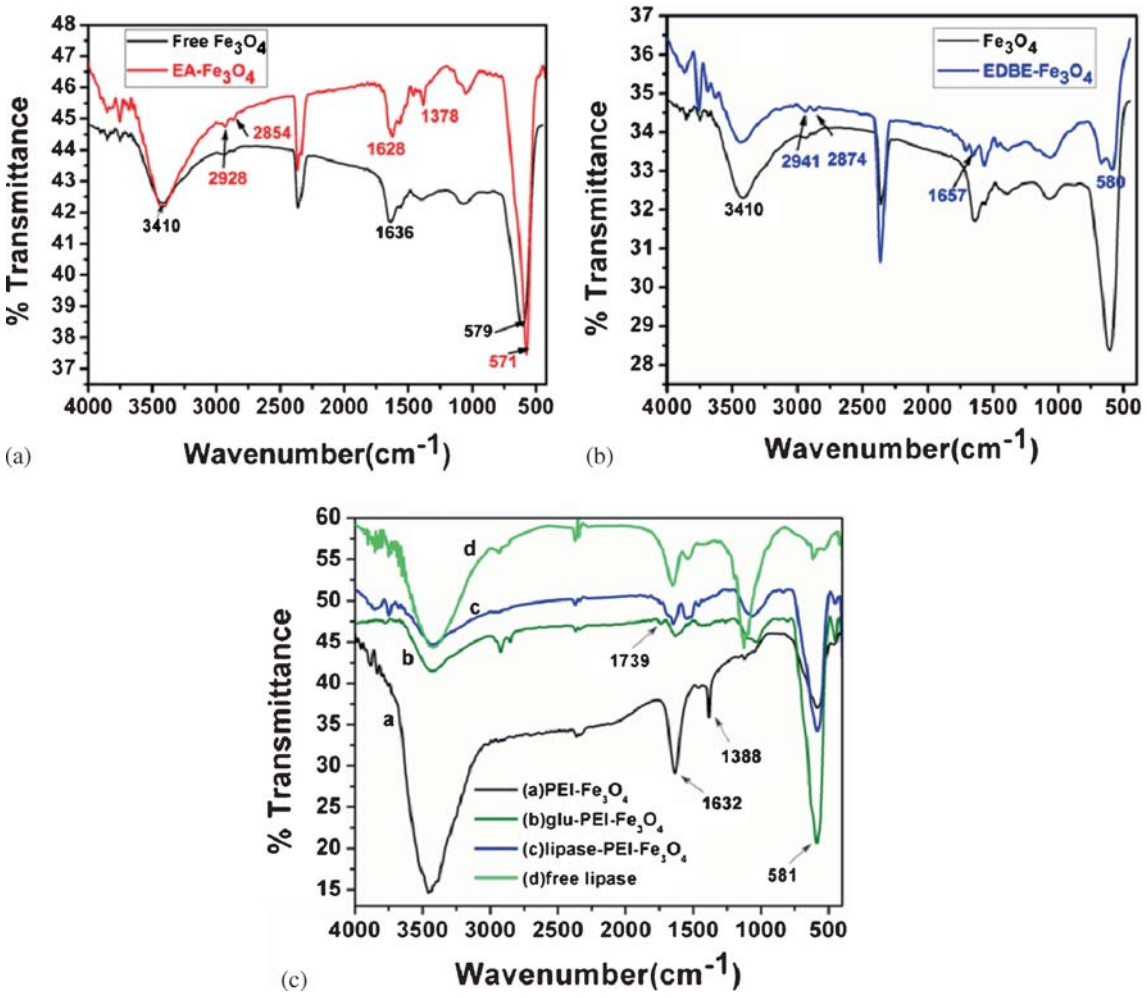

Figure 2. FTIR spectra of (a) pristine Fe_3O_4, EA-Fe_3O_4; (b) pristine Fe_3O_4 and EDBE-Fe_3O_4 nanoparticles; (c) pristine Fe_3O_4, PEI-Fe_3O_4, glutaraldehyde modified and lipase immobilized PEI-Fe_3O_4 nanoparticles.

Fe_3O_4 and EA-Fe_3O_4 are presented in Figure 2a. The aminated Fe_3O_4 (EA-Fe_3O_4) show N-H bending vibration and C-N stretching at 1628 cm^{-1} and 1378 cm^{-1}, respectively, along with the usual characteristic vibration of Fe-O at 585 cm^{-1} suggesting the introduction of surface amine moieties in a single-step solvothermal approach. In addition to all the above mentioned peaks, the two peaks observed at 2854 cm^{-1} and 2928 cm^{-1} correspond to C-H stretching vibrations. Similar to EA-Fe_3O_4, the other two aminated Fe_3O_4 nanoparticles *i.e.*, EDBE-Fe_3O_4 and PEI-Fe_3O_4 exhibited peaks corresponding to N-H bending and C-N stretching, as shown in Figures 2b and 2c, respectively. The representative FTIR spectrum for glutaraldehyde-conjugated and lipase-immobilized GLU-PEI-Fe_3O_4 is shown in Figure 2c. The peak at 1739 cm^{-1} was assigned to the -CHO functional groups on the surface of the PEI-Fe_3O_4 nanoparticles. The lipase immobilized PEI-Fe_3O_4 showed all the characteristic peaks of free lipase in addition to a peak for Fe-O at 585 cm^{-1}, hence confirming the conjugation of lipase on Fe_3O_4 nanoparticles. FTIR spectra for glutaraldehyde-conjugated and lipase-immobilized EA-Fe_3O_4 are shown in Figure S1 (Supplementary Information).

3.3 *Morphology and Size of Nanoparticles*

The morphology and size of the Fe_3O_4 nanoparticles were assessed from HRTEM and FESEM and the images of EDBE-Fe_3O_4 and EA-Fe_3O_4 are presented in Figure 3. The average size of EDBE-Fe_3O_4 (Figure 3a) nanoparticles were ~120 nm. In the case of ethanolamine used as amine modifying agent, the particles were found to be spherical in shape with an average diameter of ~70–100 nm. The corresponding HRTEM images of EA-Fe_3O_4 (Figure 3c), showed highly dispersed spherical nanoparticles which arrange to form

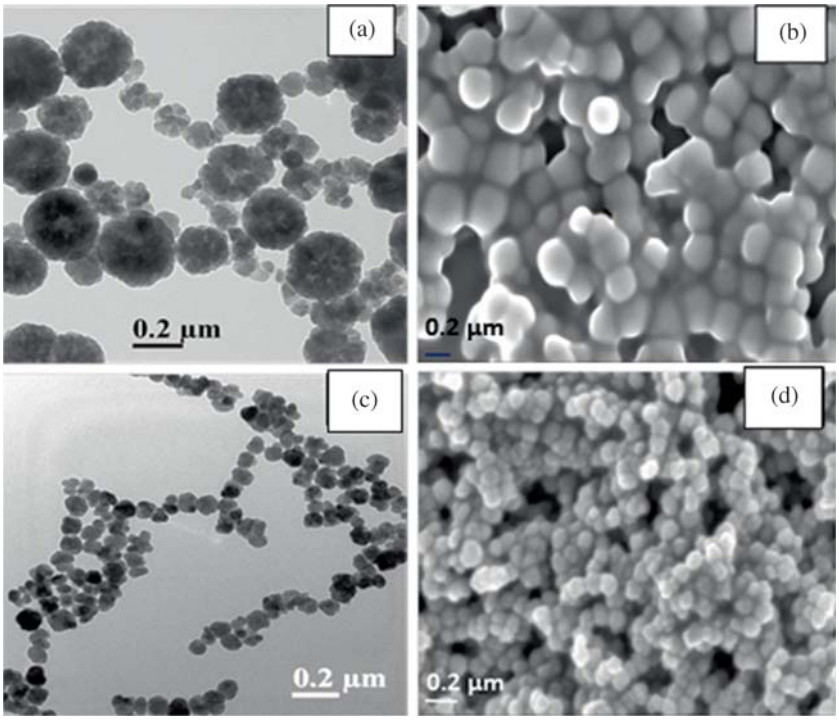

Figure 3. (a) HRTEM and (b) FESEM images of EDBE-Fe_3O_4; (c) HRTEM and (d) FESEM images of EA-Fe_3O_4.

chain like structures. Both the particles possessed smooth surface and spherical shape. The data from FESEM were nearly similar to the data obtained from HRTEM. The FESEM and TEM images of PEI-Fe_3O_4 nanoparticles are presented in Figure 4. The average particle size of PEI-Fe_3O_4 nanoparticles was found to be between 50–70 nm, the shape being nearly spherical. High magnification FESEM image showed formation of cluster type nanostructures due to aggregation between the small sized Fe_3O_4 nanoparticles. While using PEI and EDBE as surface modifying agent, the smaller nanoparticles aggregated to form nanoclusters, as reflected from their respective HRTEM and FESEM images, when EDBE was used as amine linker, the tendency to aggregate was less compared to PEI linked Fe_3O_4 nanoparticles.

3.4 *Magnetic Measurements*

Figure 5 shows the magentization behavior of the aminated magnetic nanoparticles. EA-Fe_3O_4, EDBE-Fe_3O_4 and PEI-Fe_3O_4 show superparamagnetic behavior at both 300 K and 5 K. No hysteresis loop and coercivity were observed during magnetization measurements at room temperature, although a little coercivity was observed at 5 K. The Ms values for EA-Fe_3O_4, EDBE-Fe_3O_4 and PEI-Fe_3O_4 were found to be 81, 66, and 73 emu/g, respectively at 300 K, that were lower as compared to the Ms value of pristine Fe_3O_4 obtained through solvothermal method. However, the retention of superparamagnetic property of these amine-functionalized nanoparticles facilitated easy removal of the particles using a permanent magnet.

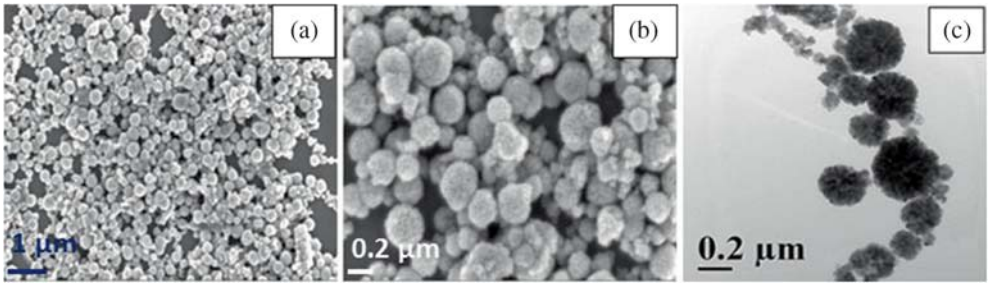

Figure 4. Low magnification (a) and high magnification (b) FESEM images, and (c) HRTEM image of PEI-Fe_3O_4 nanoparticles.

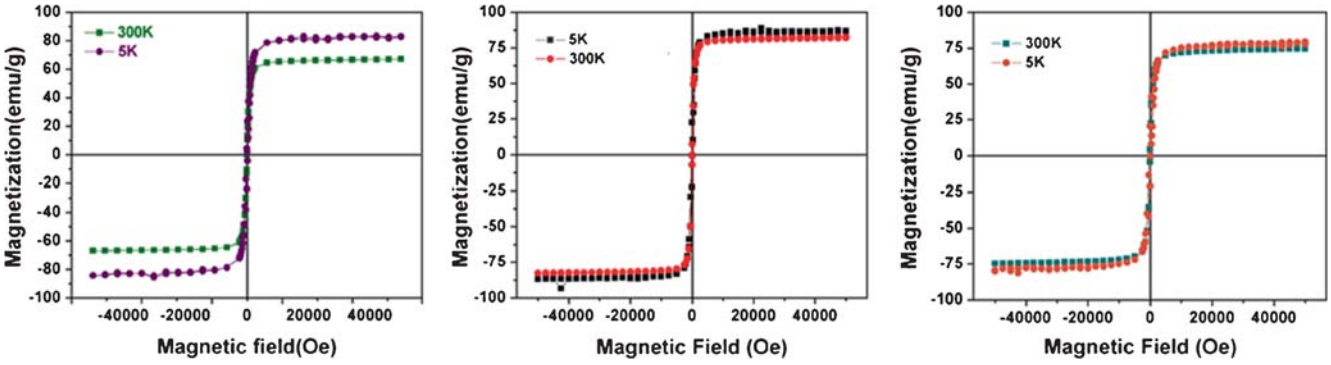

Figure 5. M-H curves at 300 K, 5 K for the amine-functionalized nanoparticles – (left) for EDBE-Fe_3O_4 nanoparticles, (middle) for EA-Fe_3O_4 nanoparticles, and (right) for PEI-Fe_3O_4 nanoparticles.

One typical M-H curve showing the stepwise conjugation of aminated Fe_3O_4 with glutaraldehyde and lipase is shown in Figure S2 (Supplementary Information). Noticeable decrease in magnetization was clearly observed on surface modification, which is probably due to the organic coating on nanoparticles. The coated Fe_3O_4 still exhibited superparamagnetism and showed a quick response to external magnetic field which was enough to easily separate the magnetic nanoparticles by using ordinary permanent magnet externally. The magnetic separation was quantitative as the remaining solution was free from the magnetic nanoparticles. Figure 6 provides a representation of the magnetic sepration procedure for the nanoparticles.

3.5 *Thermo-Gravimetric Analysis*

The step by step surface modification of the nanoparticle surface and the successive conjugation of lipase on them could be ascertained through thermo-gravimetric analysis. The TGA curves for Fe_3O_4, EDBE-Fe_3O_4, GLU-EDBE-Fe_3O_4 and lipase-EDBE-Fe_3O_4, showing the weight loss percentage vs. temperature, are given in the supplementary information (Figure S3). The TGA results showed step-wise modification of the aminated magnetic nanoparticles with gluteraldehyde followed by lipase.

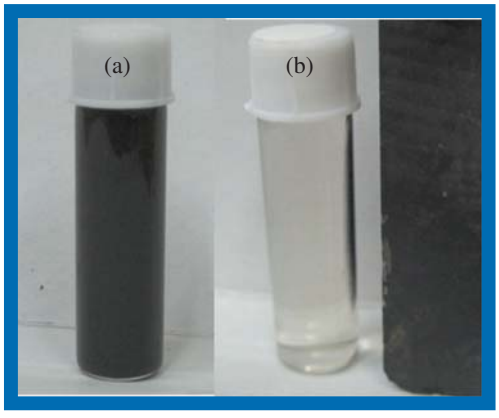

Figure 6. Picture showing (a) aqueous dispersed solution of EDBE-Fe_3O_4 nanoparticles and (b) its magnetic response to an external magnetic field placed on the right side of the vial.

3.6 *Nitrogen Adsorption-Desorption Isotherm and BET Surface Area*

The nitrogen adsorption-desorption isotherm curves and pore-size distribution curves for EDBE-Fe_3O_4, EA-Fe_3O_4, and PEI-Fe_3O_4 are shown in Figure S4 (Supplementary Information). For all the amine modified-Fe_3O_4, the isotherm pattern is of type-IV, signifying the mesoporous nature of the prepared nanoparticles with pore-size distribution in the range of 2–50 nm. Hence, it is evident that all the above nanoparticles show porous properties. The BET surface area of EDBE-Fe_3O_4, EA-Fe_3O_4 and PEI-Fe_3O_4 are 27.48, 15.57 and 14.91 m^2/g, respectively. The maximum surface area was obtained for EDBE-Fe_3O_4 due to presence of more pores inside the Fe_3O_4, which is also evident from its TEM images.

3.7 *Enzymatic Activity Study: Specific Activity of Free and Immobilized Lipase*

Effective immobilization of lipase with retention of its catalytic activity is the main objective of the present study. *Candida rugosa* lipase was immobilized on the aminated nanoparticles using glutaraldehyde coupling agent. The amount of lipase conjugated to the three different amine-modified Fe_3O_4 and the specific activities of the immobilized lipase on EA-Fe_3O_4, EDBE-Fe_3O_4 and PEI-Fe_3O_4 are presented in Table 1 (upper panel). The immobilized lipase specific activities for EA-Fe_3O_4, EDBE-Fe_3O_4 and PEI-Fe_3O_4 systems were found to be 38.4 ± 1 U/mg, 56.0 ± 2 U/mg and 37.9 ± 3 U/mg, respectively, whereas the same amount of

Table 1. Upper panel: amount of lipase immobilized on different magnetic supports using Bradford protein assay and the specific activity of immobilized lipase. Data obtained are the mean of three different sets of experiments. Lower panel: Temperature stability of free lipase and lipase-EDBE-Fe_3O_4 (relative activity at various temperatures).

Lipase immobilized Fe_3O_4 support	Total enzyme loading (μg enzyme per mg nanoparticle)	Specific activity (U/mg enzyme)
Free lipase	20 μL (1 mg mL^{-1})	66.7 ± 1
EDBE-Fe_3O_4	4.0 ± 0.05	56.0 ± 2
EA-Fe_3O_4	3.5 ± 0.03	38.4 ± 1
PEI-Fe_3O_4	3.2 ± 0.02	37.9 ± 3
Temperature (°C)	Free lipase Relative activity (%)	Immobilized lipase Relative activity (%)
50	89.2	89.9
60	83.5	93.5
70	65.3	90.5
80	41.6	89.1

free lipase showed higher specific activity of about 66.74 U/mg under the same specified condition. The highest activity observed for EDBE-Fe_3O_4 system was possibly due to a lesser chance of distortion as it is conjugated to Fe_3O_4 through a longer hydrophilic linker. Increased space between the support and the lipase possibly resulted in perfect retention of the catalytic site. As the highest recovery of activity was achieved in case of EDBE as surface modifying and nanoparticle stabilizing agent, the other enzymatic studies were performed on lipase immobilized on EDBE-Fe_3O_4.

3.8 *Specific Activities of Two Different Lipases - Units 807 U/mg (HU) and 2.45 U/mg (LU)*

Two different lipases, one higher unit (HU), and another lower unit (LU), were immobilized on EDBE-Fe_3O_4 and their catalytic activities were compared. Table S1 (Supplementary Information) displays the specific activities of HU lipase and LU lipase immobilized on EDBE-Fe_3O_4. The HU lipase immobilized on EDBE-Fe_3O_4 showed more activity compared to LU lipase.

3.9 *Temperature Stability of Immobilized Lipase*

The temperature stabilities of the free and immobilized lipase (HU) on EDBE-Fe_3O_4 nanoparticles were studied, as shown in Table 1 by their specific activity values recorded at different temperatures (lower panel). It shows that the immobilized lipase exhibited higher catalytic activity at all temperatures compared to free lipase under similar experimental conditions. The higher temperature stability of immobilized lipase may be due to its restricted conformational mobility resulting from rigid covalent conjugation of lipase on the solid magnetic support.[27,28] Jiang *et al.*, reported that the immobilized lipase retains only 60% of its initial activity at 60°C.[29] In our studies, we have observed that the immobilized lipase retains 89% of its initial activity at 80°C.

3.10 *Kinetic Parameters of Free and Immobilized Lipase*

The kinetic parameters of the free and immobilized lipase were obtained from Lineweaver-Burk double reciprocal plot by varying the substrate (S) concentration at constant temperature and pH. The reciprocal of substrate concentration was plotted against the reciprocal of reaction rate (V) for both the free and immobilized lipase, as shown in Figure 7. Both the

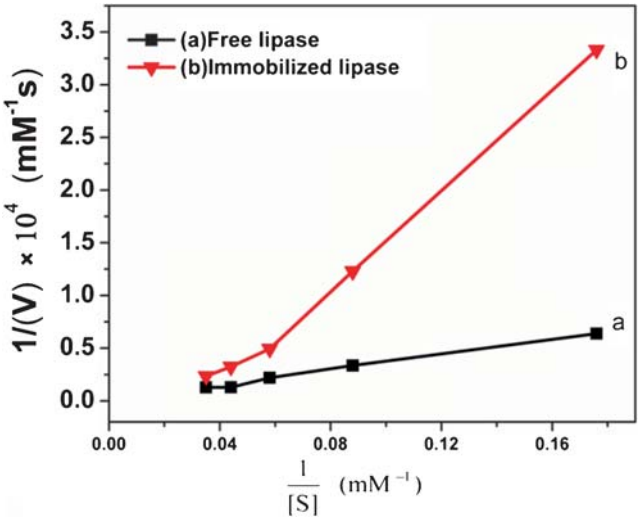

Figure 7. Lineweaver-Burk plot for (a) free lipase and (b) immobilized lipase on EDBE-Fe_3O_4 nanoparticles where V and S are reaction rate and substrate concentration, respectively.

free and immobilized lipase obeyed Michaelis-Menten enzyme kinetics, with the apparent Michaelis-Menten constant (K_m) calculated to be 141.7 and 145.4 mM, respectively. K_m of the enzyme is related to its affinity towards the substrate. The higher the value of K_m, lower will be the affinity to substrate and vice-versa. Here, the K_m value was seen to increase upon immobilization, as a relatively higher K_m value was observed for the immobilized lipase than the free enzyme, similar to those reported in literature.[16,30,31] However, it can be clearly seen that the difference between K_m for both the free and immobilized enzyme on EDBE-Fe_3O_4 nanoparticles is very small. So, the nanoparticle support reported in this work is a promising carrier for enzyme loading and recycling of catalyst.

3.11 *Reusability of Immobilized Lipase*

The most important benefit of immobilized lipase is recycling of the enzyme which is extremely important for industrial applications. For each iterative cycle, the immobilized lipase was checked for activity measurement. After every catalytic operation, the immobilized lipase was washed with PBS buffer, magnetically recovered (as shown in Figure 6), and checked for subsequent activity. The activity of immobilized lipase after successive cycles relative to the first cycle is shown in Figure 8. The immobilized lipase was seen to retain most of initial catalytic activity. For example, even after seven cycles the activity of the immobilized lipase retained about 90% of initial value. The reusability, recyclability, and easy recovery make enzyme-immobilized on MNPs a robust biocatalyst for future industrial application.

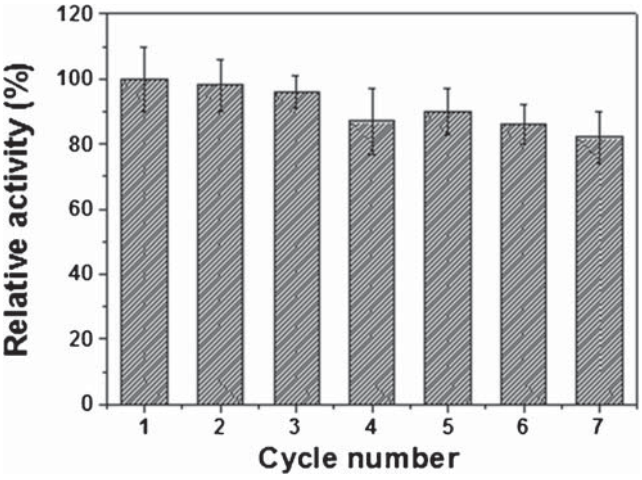

Figure 8. Reusability data for EDBE-Fe_3O_4 nanoparticles with immobilized lipase. Relative activity data are with respect to the first cycle data.

4. Conclusions

In this study, Fe_3O_4 nanoparticles bearing surface amine groups were prepared by a one-step facile chemical method. These Fe_3O_4 nanoparticles were monodisperse, as evident from their TEM images. Lipase was successfully immobilized onto the MNPs through covalent linking with the surface functional group. The maximum activity of the immobilized enzyme was observed in case of EDBE linker, and it retained 83.9% of activity compared to the same amount of free lipase. The study of activity as a function of temperature revealed that the immobilized lipase-EDBE-Fe_3O_4 retained most of its initial activity at higher temperatures as compared to the corresponding free lipase, signifying greater thermal stability of the immobilized lipase. Moreover, the immobilized lipase retained about 90% of their initial activity even after seven times recycling. In a nut-shell, we have demonstrated an inexpensive strategy for the formation of high purity amine-functionalized MNPs and utilized them for immobilization of an industrially important enzyme *viz*. lipase. Such immobilization results in retention of the most of initial catalytic activity, thermal stability and enhanced recyclability of lipase, thereby increasing their effectiveness from the view point of cost and environmental viability that are extremely important in any industrial process.

Supplementary Information (SI)

FTIR spectra, M-H curve showing the stepwise conjugation of aminated Fe_3O_4 with glutaraldehyde and lipase, comparison of specific activity of lipase-EDBE-Fe_3O_4, thermogravimetric data, nitrogen adsorption-desorption isotherm curves are provided in the Supplementary Information. Supplementary Information is available at www.ias.ac.in/chemsci.

Acknowledgements

Authors thank SRIC, IIT Kharagpur for financial support (project code NPA, institute approval number - IIT/SRIC/CHY/NPA/2014-15/81).

References

1. Konwarh R, Karak N, Rai S K and Mukherjee A K 2013 *Nanotechnology* **20** 225107
2. Ghavami M, Koohi M and Kassaee M Z 2013 *J. Chem. Sci.* **125** 1347
3. Wang W, Xu Y, Wang D I C and Li Z 2009 *J. Am. Chem. Soc.* **131** 12892
4. Hartmann M and Jung D 2010 *J. Mater. Chem.* **20** 844
5. Raghava S, Singh P K, Rao A R and Gupta M N 2009 *J. Mater. Chem.* **19** 2830

6. Chao C, Liu J, Wang J, Zhang Y, Zhang B, Zhang Y, Xiang X and Chen R 2013 *ACS Appl. Mater. Interfaces* **5** 10559
7. Mahmoud K A, Lam E, Hrapovic S and Luong J H T 2013 *ACS Appl. Mater. Interfaces* **5** 4978
8. Zhang Y, Yang Y, Ma W, Guo J, Lin Y and Wang C 2013 *ACS Appl. Mater. Interfaces* **5** 2626
9. Hritcu D, Dodi G, Silion M, Popa N and Popa M I 2011 *Polym. Bull.* **67** 177
10. Cui Y, Li Y, Yang Y, Liu X, Lei L, Zhou L and Pan F 2010 *J. Biotechnol.* **150** 171
11. Pan B F, Gao F and Gu H C 2005 *J. Colloid Interf. Sci.* **284** 1
12. Xie W and Ma N 2009 *Energy Fuels* **23** 1347
13. Chen Z, Xu W, Jin L, Zha J, Tao T, Lina Y and Wang Z 2014 *J. Mater. Chem. A* **2** 18339
14. Cho E J, Jung S, Lee K, Lee H J, Nam K C and Bae H J 2010 *Chem. Commun.* **46** 6557
15. Sahoo B, Sahu S K and Pramanik P 2011 *J. Mol. Catal. B: Enzym.* **69** 95
16. Gelbrich T, Reinartz M and Schmidt A M 2010 *Biomacromolecules* **11** 635
17. Kim H, Kwon H S, Ahn J, Lee C-H and Ahn I S 2009 *Biocatal. Biotransfor.* **27** 246
18. Shen W, Ren L, Zhou H, Zhang S and Fan W 2011 *J. Mater. Chem.* **21** 3890
19. Betigeri S S and Neau S H 2002 *Biomaterials* **23** 3627
20. Dhake K P, Tambade P J, Qureshi Z S, Singhal R S and Bhanage B M 2013 *ACS Catalysis* **1** 316
21. Sakai S, Yamaguchi T, Watanabe R, Kawabe and Kawakami K 2011 *Catal. Commun.* **11** 576
22. Chiou S H and Wu W T 2004 *Biomaterials* **25** 197
23. Ren S Y, Rivera J G, He L, Kulkarni H, Lee D K and Messersmith P B 2011 *BMC Biotechnology* **11** 63
24. Lee D J, Ponvel K M, Kim M, Hwang S, Ahn I S and Lee C H 2009 *J. Mol. Catal. B- Enzym.* **57** 62
25. Jiang Y, Guo C, Xia H, Mahmood I, Liu C and Liu H 2009 *J. Mol. Catal. B- Enzym.* **58** 103
26. Zor T and Selinger Z 1996 *Anal. Biochem.* **236** 302
27. Yu B Y and Kwak S Y 2010 *Dalton Trans.* **40** 9989
28. Sui Y, Cui Y, Nie Y, Xia G M, Sun G X and Han J T 2012 *Colloids Surf., B* **93** 24
29. Jiang Y, Guo C, Xia H, Mahmood I, Liu C and Liu H 2009 *J. Mol. Catal. B-Enzym.* **58** 103
30. Bayramoglu G, Metin A U, Altıntas B and Arıca M Y 2010 *Biores. Technol.* **101** 6881
31. Ye P, Xu Z K, Wu J, Innocent C and Seta P 2006 *Biomaterials* **27** 4169